Experimental and Numerical Investigations of Effects of Wall Friction and Vibrational Amplitude on Convection Phenomena in Granular Materials Under Vertical Vibrations

Tanapon Yachai, Itthichai Preechawuttipong, and Pawarut Jongchansitto

1 Introductions

In the engineering context, granular materials can be defined as a cluster of solid particles, whose macroscopic behaviors are controlled by the interaction forces between particles, for example, rock, soil, sand, plastic pellets, pharmaceuticals, etc. Indeed, particle mixing and segregation often occur in many industrial processes involved the transportation and handling of granular mixtures under vibrated or shaken systems. Convection is one of key driving mechanism for such phenomena (Windows-Yule et al. 2013, 2014; Windows-Yule 2016). The strength of the granular convection depends on many parameters such as number of particles (Windows-Yule et al. 2013, 2014; Windows-Yule 2016), aspect ratio of container dimensions (Windows-Yule and Parker 2014; Hsiau et al. 2011), material properties (Windows-Yule et al. 2013, 2014), dimensionless vibrational acceleration (Γ) (Zhang et al. 2014), and wall friction (Song and Zhang 2020). Among these parameters, the wall friction dominates compared to the others (Windows-Yule and Parker 2014; Then et al. 2020). Only, a few previous studies considered the strength of convection due to the friction coefficient between particle and wall container. Grossman (Grossman 1997) numerically examined the effects of boundary conditions on convection in vibrated granular systems. The results showed that the net shear force exerted by the walls on the particles determines the strength and direction of the convection rolls. Hsiau et al. (2002) and Zeilstra et al. (2008) performed experiments and simulations to investigate the effect of sidewalls roughness on the convection under vertically vibrated granular bed. The results showed that the strength of the convection increases with the sidewalls roughness. Nevertheless, the effect of the particle–wall friction on convection

T. Yachai (✉) · I. Preechawuttipong · P. Jongchansitto
Department of Mechanical Engineering, Faculty of Engineering, Chiang Mai University, 239 Huay Kaew Rd., Muang 50200, Chiang Mai, Thailand
e-mail: tanapon_ya@cmu.ac.th

R. K Agarwal (ed.), *Recent Advances in Manufacturing Engineering and Processes*, Lecture Notes in Mechanical Engineering,
https://doi.org/10.1007/978-981-19-6841-9_13

phenomena has been still unclear. Therefore, the present study is aimed to investigate the influence of wall friction and vibrational amplitude on convection phenomena in a vertically vibrated granular system by means of experiments and reproduced numerical simulations.

2 Methodology

The experiment and simulation setup as well as the analysis of convection through the dimensionless angular velocity is presented in this section.

2.1 Experimental Setup

Figure 1A shows a preparation of our experiments. A particle was made from the polymethyl methacrylate (PMMA). The particle has a mean diameter (D_m) of 10 mm and a thickness of 5 mm. The particle density obtained from the supplier datasheet is 1190 kg/m^3. Each particle was then randomly placed inside the container covering the front and back sides by a clear PMMA sheet, as shown in Fig. 1b. The aspect ratio between bed height and bed width was equal to 1. A granular sample consisted of 4000 particles with a uniform distribution of five different diameter sizes $D \in$ [9.0, 9.5, 10.0, 10.5, 11.0] mm. A fluorescent sticker with the diameter of 5 mm was also attached to each particle. This sticker is glowed in the dark under UV light, as presented in Fig. 1c. Note that the center of the sticker was coincident to the centroid of the particle. This is very novel and useful technique for extracting the location of the particles from an image processing. To vary the coefficient of friction between particle and wall container, seven types of materials consisting of a polytetrafluoroethylene (PTFE) tape, a polyethylene (PE) tape, a masking tape, a sandpaper No. 10, 000, a sandpaper No. 5000, and a polyurethane (PU) tape were attached to the sidewalls of the container. These materials provide the coefficient of the particle–wall friction $\mu_w \in$ [0.15, 0.26, 0.36, 0.46, 0.61, 0.81, 0.95], respectively. The coefficient of interparticle friction (μ_p) is equal to 0.5. Note that μ_w and μ_p were obtained from the measurement based on the ASTM D4918-97 standard (ASTMD4918-97 2007).

The granular sample under a gravity was subjected to a vertical vibration with a sinusoidal wave. The vertical vibration was provided by a vertical testing machine through a scotch-yoke mechanism, as shown in Fig. 1a. The level of vibration was controlled by dimensionless acceleration (Γ). The dimensionless acceleration can be defined as $\Gamma = A\omega^2/g$, where g is the gravity, A is the vibrational amplitude, and $\omega = 2\pi f$ is the vibrational frequency. In this study, the dimensionless acceleration was fixed at 5 for a chaotic state of granular system (Chen 2020), while the vibrational frequency was adjusted suitable for the vibrational amplitude of $0.5D_m$ and $1.0D_m$, respectively. During the experiments, the center of each particle was recorded by a high-speed camera with 240 fps. Each considered frame of the video was used to

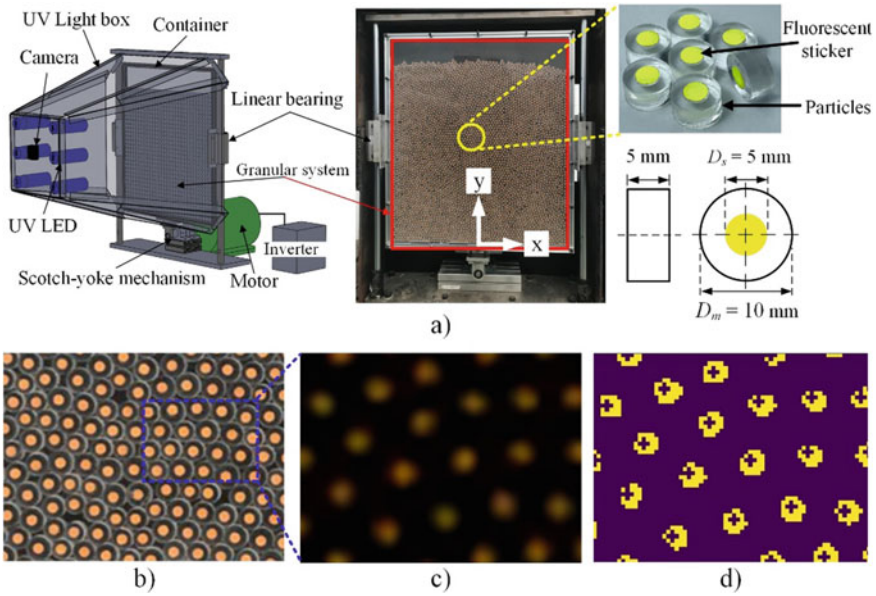

Fig. 1 **a** Experimental preparation and sample of tested particles. **b** A snapshot of granular sample under visible light. **c** A snapshot of granular sample under UV light. **d** Result obtained from image processing. Note that the plus sign represents the center of the particle

extract the location of the particle center by an image processing technique. Figure 1d presents the obtained image after performing the image processing.

2.2 Numerical Setup

The simulations were carried out by means of the non-smooth contact dynamics (NSCD) method, which was originally developed by Moreau and Jean (Jean 1999). This method is suitable for simulating large assemblies of rigid massive particles. In this method, the equations of motion (i.e., Newton's second laws) are integrated over a small-time step and combined with the kinematic constraints resulting from contact interactions. An open-source software named "LMGC90" (http://mimetics-engineering.fr/index.php/en/lmgc90-2/), which was developed in Montpellier, was used for the simulations in this study. The 2D simulations were compared with the experiments under the same conditions. The experiments and simulations were performed up to 300 s. The time step of simulation used for updating the particle position was set to $1/2^7$ fs. For a comparison between experiments and simulations, an average velocity field was plotted to reveal the convection. The average velocity field can represent the motion of each particle corresponding to the flow behavior of granular media. To determine the average velocity field, the center locations of

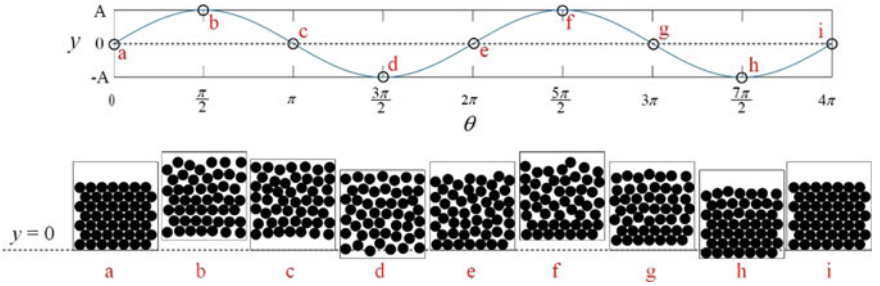

Fig. 2 Schematic of a phase of vibration corresponding to the sinusoidal wave. Note that the dotted line is the reference line of the container movement

each particle at each phase of 4π were exported every 4 s. It is clearly seen that the selected phase of 4π is the highest compaction after a rearrangement of the particles, as illustrated in Fig. 2. These locations were then employed to compute the velocity of each particle for every 4 s. Eventually, the average velocity field was determined by averaging all the velocity data for 300 s.

2.3 Dimensionless Angular Velocity (W)

In the previous studies, the granular temperature (T) (Windows-Yule and Parker 2014) and the dimensionless convection flow rate (J) (Windows-Yule 2016) are commonly applied as the indicators to describe the quantity of convection. The granular temperature is used to quantify the kinetic energy of the flow, while the dimensionless convection flow rate is used to quantify the mass flow rates at the horizontal plane crossing the center of convection. However, the major disadvantage of both indicators is that they cannot explain the direction of convection and the convection at low velocity. Therefore, the dimensionless angular velocity (W) was introduced in the present study to describe the quantity of the strength convection. The dimensionless angular velocity is defined as the ratio of the angular velocity of the convection to the angular frequency of the sinusoidal wave of vibration, which can be expressed as:

$$W = \frac{W_{\mathrm{L}} + W_{\mathrm{R}}}{2\omega} \tag{1}$$

where W_{L} and W_{R} are the average angular velocity of the left and right convection rolls, respectively. The center of rotation for each convection roll can be obtained under the concept that a point having the highest number of velocity vectors rotating around that point, as represented by the blue circle in Fig. 3a. The W_{L} and W_{R} can be determined by:

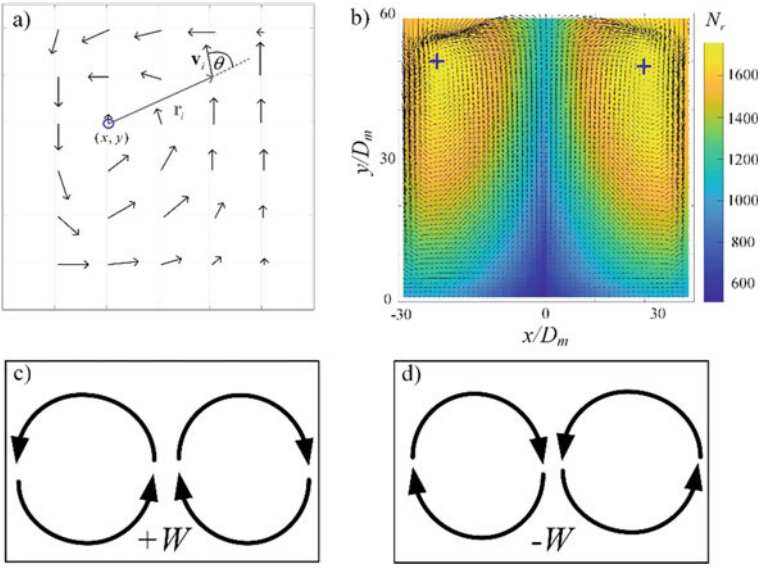

Fig. 3 **a** An illustration of a velocity field for determination of the center of the convection. **b** The number of vectors rotating around point (N_r). **c** An illustration of the normal convection. **d** An illustration of the reverse convection

$$W_L = \frac{\sum_{i=1}^{N_L} \left(\frac{|\mathbf{v}_i| \sin\theta}{|\mathbf{r}_i|} \right)}{N_L} \text{ and } W_R = \frac{\sum_{i=1}^{N_R} \left(\frac{|\mathbf{v}_i| \sin\theta}{|\mathbf{r}_i|} \right)}{N_R} \tag{2}$$

where N_L and N_R are number of vectors on left and right convection roll, respectively. θ is the smallest angle between the magnitude of a radial vector $|\mathbf{r}_i|$ the magnitude of a velocity vector $|\mathbf{v}_i|$ of ith vector. The term of $\sin\theta$ is positive when $\mathbf{v}_i$ rotates counterclockwise about the considered point. On the other hand, $\sin\theta$ is negative when $\mathbf{v}_i$ rotates clockwise about the considered point. Figure 3b shows a surface plot of the number of vectors rotating about each considered point. Two blue crosses represent the center of the convection having the highest number of rotating vectors. Hence, W varies from -1 to 1. The dimensionless angular velocity is equal to 1, corresponding to the largest strength of the normal convection, as shown in Fig. 3c. On the contrary, the largest strength of the reverse convection (see in Fig. 3c) exhibits when $W = -1$. When the dimensionless angular velocity is close to 0, it means that the convection does not occur.

3 Results

In this section, experimental and simulation results of the convection due to the effects of the wall friction and the vibrational amplitude are discussed.

3.1 *Effect of the Wall Friction*

Figure 4A shows the evolution of the dimensionless angular velocity (W) as function of the particle–wall friction obtained from the experiment and simulation results for both the vibrational amplitude of $0.5D_{\mathrm{m}}$ and $1.0D_{\mathrm{m}}$. The trend of both experiment and simulation results is well correlated. It can be said that the dimensionless angular velocity starts to increase and then stabilizes at a constant value after $\mu_{\mathrm{w}} > 0.6$. Figure 4b presents the average velocity fields of points a, b, and c at different levels of μ_{w}. For $\mu_{\mathrm{w}} < 0.26$, it was observed that the convection does not appear, i.e., $W \approx 0$. The strength of the convection then tends to increase with μ_{w} until reached its maximum value. Finally, the strength of the convection is steady after $\mu_{\mathrm{w}} > 0.6$. It was also found that the magnitude of the dimensionless angular velocity for the experiments is slightly greater than that for the simulations. This can be explained by the front and rear covers of the container used in the experiments affect to the flow behavior in granular system, which is consistent to the previous study (Fortini and Huang 2015).

Let us consider the strength of the convection when $\mu_{\mathrm{w}} > \mu_{\mathrm{p}}$, it is clearly seen that only the effect of the particle–wall friction cannot cause an enhancement of the dimensionless angular velocity. Therefore, the particle at the container wall is required the interparticle friction from an adjacent particle to migrate downward into

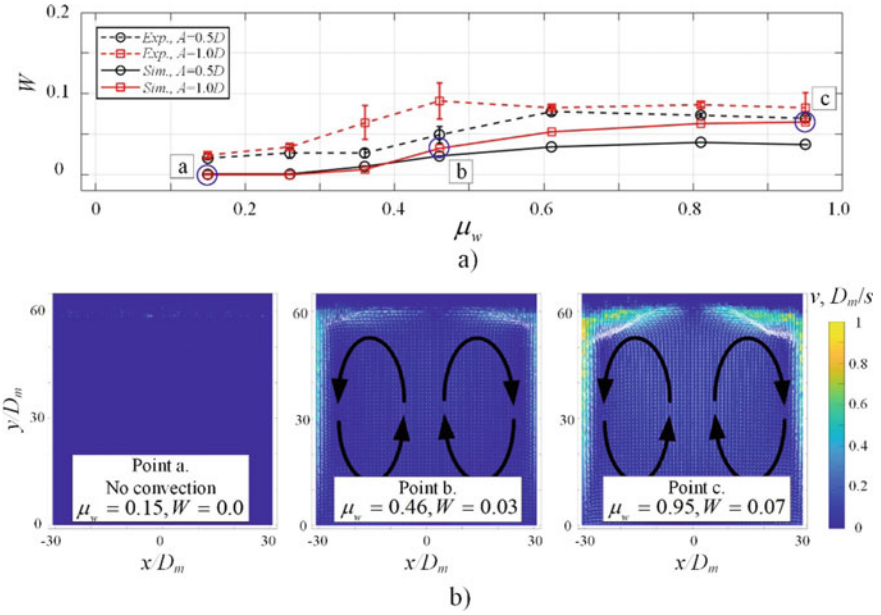

Fig. 4 **a** Dimensionless angular velocity as a function of the particle–wall friction obtained from experiments and simulations for the vibrational amplitude of $0.5D_{\mathrm{m}}$ and $1.0D_{\mathrm{m}}$. **b** Examples of the average velocity field of points **a**–**c** corresponding to Fig. 4a

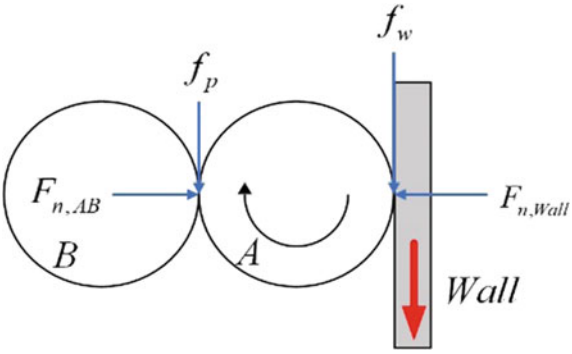

Fig. 5 Free-body diagram of particles at the container wall while the container is moving down

the bottom of the container (Song and Zhang 2020). This can be explained by a free-body diagram, as illustrated in Fig. 5, where $F_{\mathrm{n,\,wall}}$ is the normal force acting by the container wall, f_{w} is the particle–wall friction force, $F_{\mathrm{n,\,AB}}$ is the normal force between particle *A* and particle *B*, and f_{p} is the friction force between particle *A* and particle *B*.

3.2 Effect of the Vibrational Amplitude

It was observed that when the vibrational amplitude was increased, the strength of the convection is increased for any μ_w. This is due to the fact that larger vibrational amplitude provides the larger displacement of the container, thus leading to more spaces between the particles for the movement (Zhang et al. 2014; ASTMD4918-97 2007). Time for the particle movement is also increased when the vibrational amplitude was increased, thus causing the higher velocity. Comparison with the simulations, the strength of the convection due to the vibrational amplitude obtained from the experiment's overestimates for any μ_{w}.

4 Conclusion

This work pointed out the first step for a better understanding of the effect of the wall friction and the vibrational amplitude on convection phenomena in 2D granular system under vertical vibration. The appearance and the strength of convection mechanisms were characterized by the dimensionless angular velocity (W). All cases of an occurrence of the convection were normal. The convection started to occur when the wall friction $\mu_{\mathrm{w}} > 0.26$ and then reached to the maximum for μ_{w} close to μ_{p}. The strength of convection was no longer increased for $\mu_{\mathrm{w}} > \mu_{\mathrm{p}}$ because the particles rotated about itself. In addition, the convection was much clearer when the vibrational amplitude was increased. It must be noted that the experimental and numerical

results are correlated, but an underestimation of the results by the simulation was observed. The contribution of this work can be considered as the basic data for the segregation and mixing of the binary materials.

Acknowledgements This work was supported by TA/RA Scholarships from Graduate School, Chiang Mai University and Graduate Research Assistant Scholarships from Faculty of Engineering, Chiang Mai University.

References

ASTMD4918-97 (2007)
Chen B.: Powder Technol. **363**, 575–583 (2020)
Fortini, A., Huang, K.: Phys. Rev. E **91**, 032206 (2015)
Grossman, E.: Phys. Rev. E **56**, 3290 (1997)
Hsiau, S., Wang, P., Tai, C.: AICHE J. **48**, 1430–1438 (2002)
Hsiau, S., Liao, C., Sheng, P., Tai, S.: Exp. Fluids **51**, 795–800 (2011)
Jean, M.: Comput. Method. Appl. M **177**, 235–257 (1999)
LMGC90 Homepage. http://mimetics-engineering.fr/index.php/en/lmgc90-2/
Song, X., Zhang, G.: Powder Technol. **372**, 40–47 (2020)
Then, H., Sekiguchi, T., Okumura, K.: Soft Matter **16**, 8612–8617 (2020)
Windows-Yule, C.: New. J. Phys. **18**, 033005 (2016)
Windows-Yule, C., Parker, D.: Powder Technol. **261**, 133–142 (2014)
Windows-Yule, C., Rivas, N., Parker, D.: Phys. Rev. Lett. **111**, 038001 (2013)
Windows-Yule, C., Weinhart, T., Parker, D., Thornton, A.: Phys. Rev. E **89**, 022202 (2014)
Zeilstra, C., et al.: Powder Technol. **184**, 166–176 (2008)
Zhang, F., Wang, L., Liu, C., Wu, P., Zhan, S.: Phys. Lett. A **378**, 1303–1308 (2014)